Spectroscopy of "Big Trio" Objects Using the "Scorpio" Spectrograph of the 6-m Telescope of the Special Astrophysical Observatory *

Yu. N. Parijskij[1], A. I. Kopylov[1], A. V. Temirova[2], N. S. Soboleva[2], O. P. Zhelenkova[1], O V. Verkhodanov[1], W. M. Goss[3], T. A. Fatkhullin[1]

[1] Special Astrophysical Observatory, Russian Academy of Sciences, Nizhnij Arkhyz, Karachaj-Cherkessian Republic, 357147 Russia
[2] St. Petersburg Branch of the Special Astrophysical Observatory, Russian Academy of Sciences, Pulkovskoe sh. 65, St. Petersburg, 196140 Russia
[3] National Radio Astronomy Observatory, P. O. Box O, 1003 Lopezville Road, Socorro, NM 87801-0387, USA

Received February 1, 2010; accepted February 5, 2010.

Abstract. We present the results of spectroscopy of 71 objects with steep and ultra-steep spectra ($\alpha < -0.9$, $S \propto \nu^{\alpha}$) from the "Big Trio" (RATAN-600–VLA–BTA) project, performed with the "Scorpio" spectrograph on the 6-m telescope of the Special Astrophysical Observatory (Russian Academy of Sciences). Redshifts were determined for these objects. We also present several other parameters of the sources, such as their Rmagnitudes, maximum radio sizes in seconds of arc, flux densities at 500, 1425, and 3940 MHz, radio luminosities at 500 and 3940 MHz, and morphology. Of the total number of radio galaxies studied, four have redshifts $1 < z < 2$, three have $2 < z < 3$, one has $3 < z < 4$,and one has $z = 4.51$. Thirteen sources have redshifts $0.7 < z < 1$ and 15 have $0.2 < z < 0.7$. Of all the quasars studied, five have redshifts $0.7 < z < 1$, seven have $1 < z < 2$, four have $2 < z < 3$, and one has $z = 3.57$. We did not detect any spectral lines for 17 objects.
DOI: 10.1134/S1063772910080019

* ISSN 1063-7729, Astronomy Reports, 2010, **54**, Iss.8, 675-695.
Original Russian Text (C) Astronomicheskij Zhurnal, 2010,**87**, No.8, 739-759.

1. INTRODUCTION

The "Big Trio"5 project, which was initiated in 1991-1992 [1] and is based on three large instruments — the RATAN-600, the VLA, and the 6-m optical telescope of the Special Astrophysical Observatory (SAO) – is aimed at searching for and studying very distant radio galaxies. (For a detailed description of the project, see the book by Verkhodanov and Pariiskii [2].) The project was carried out in several stages. The first stage – a search survey with the RATAN-600 radio telescope in 1980-1981 (the "Kholod" experiment [3, 4]) – resulted in the RC catalog [5, 6] at 3940 MHz, which also made use of the Texas catalog at 365 MHz [1] to obtain a sample the Texas catalog at 365 MHz1 to obtain a sample of objects with steep and ultra-steep spectra. (The steepness of the radio spectrum was already known to be useful for selecting very distant objects [7, 8].)

The next stage was to study the structure of the sample objects with the VLA at 1425 and 4885 MHz. This made it possible to identify FRII sources – the most energetic radio galaxies, associated with gE giant elliptical galaxies - and to improve their coordinates.

The third stage was optical identification of the radio sources: for bright sources, from the Palomar prints and, for fainter ones, from R-band observations with the 6-m telescope of the SAO [9-11]. We studied the optical structures of some objects with a resolution of <1" using the NOT (Nordic Optical Telescope, Canary Islands) [12].

To derive the spectral energy distributions of the host galaxies based on evolutionary models, the fourth stage included BVRI-photometry with the 6-meter SAO telescope [13, 14]. These data were used to obtain photometric redshifts and estimate the ages of the host galaxies.

In the last stage, we determined spectroscopic redshifts, first with the multi-pupil spectrograph [15] and then with the "Scorpio" spectrograph (mounted on the 6-m telescope of the SAO) [16].

The results for all previous stages were published earlier [9–27]. In this paper, we present the results of the last stage: spectoscopic redshifts derived from observations with the "Scorpio" spectrograph (on the 6-m telescope of the SAO).

2. OBSERVATIONAL RESULTS

The data obtained from our observations with the "Scorpio" spectrograph mounted on the 6-m SAO telescope are collected in four tables. In total, we studied 71 objects with steep and ultra-steep spectra from the RC catalog. These include 17 quasars, with the other objects being radio galaxies. Tables 1 and 2 present the results for radio galaxies with detected emission lines, subdivided according to their redshifts. Table 1 contains 22 radio galaxies with redshifts z¿0.7,and Table 2 – 15 radio galaxies with redshifts between 0.2 and 0.7.

The columns of Tables 1 and 2 contain for each object: 1 — a running number; 2 —- the name in the RC catalog; 3, 4 — the right ascension and declination of the object for equinox 2000; 5 — the R-band magnitude; 6 — the spectroscopic redshift (z_{sp}); 7 — the largest angular size in arcseconds, LAS; 8, 9, 10 — the flux densities S, in mJy, at 3940, 1400, and 500 MHz (the last obtained from interpolating the spectrum); 11, 12 — the spectral indices α ($S \propto \nu^{\alpha}$) at 3940 and 500 MHz; 13, 14 — the luminosities L, W Hz^{-1}, at 3940 and 500 MHz; 15 — the radio source morphology, with 'P' denoting a point-like object, 'D' a double

[1] Kindly provided by Prof. J. Douglas prior to its publication.

Table 1. Radio galaxies with $z > 0.7$.

No.	RCJ name	RA	Dec	m_R	z_{sp}	LAS	S_{3940} mJy	S_{1400} mJy	S_{500} mJy
1	2	3	4	5	6	7	8	9	10
1	0015+0501	$00^h15^m22.8^s$	05°01'22.4"	23.2	0.813	20.1"	34	110	295
2	0034+0513	00 34 06.24	05 14 57.6	23.3	0.962	12.1	93	252	605
3	0105+0501	01 05 34.46	05 01 09.8	22.8	3.138	7.6	27	92	285
4	0213+0516	02 13 36.25	05 18 19.2	22.1	0.935	36.8	143	425	963
5	0225+0506	02 25 09.75	05 08 37.4	22.1	0.770	0.2	82	239	586
6	0311+0507	03 11 47.99	05 08 04.1	22.9	4.514	2.8	135	537	1711
7	0444+0501	04 44 17.93	05 01 25.7	23.0	1.820	11.1	70	206	553
8	0506+0508	05 06 25.00	05 08 19.3	21.6	0.817	0.8	91	221	427
9	0744+0500	07 44 52.63	05 00 09.4	>24.5	2.48	10.8	28	99	341
10	0837+0446	08 37 29.37	04 44 21.8	22.2	1.769	3.9	62	164	384
11	0909+0445	09 09 51.09	04 44 22.9	20.6	0.753	0.1	70	192	472
12	1322+0449	13 22 03.48	04 48 50.5	20.4	0.799	1.7	46	115	269
13	1339+0445	13 39 37.85	04 55 04.3	22.3	0.740	34.0	40	126	290
14	1357+0453	13 57 37.39	04 53 16.1	21.3	0.864	12.4	91	250	584
15	1503+0456	15 03 59.70	04 56 50.4	22.8	0.788	4.5	64	199	545
16	1510+0438	15 10 12.67	04 39 31.5	22.1	0.870	3.4	71	154	318
17	1626+0448	16 26 50.29	04 48 51.3	22.9	2.656	2.4	57	200	564
18	1638+0450	16 38 32.21	04 49 56.3	22.3	1.272	1.9	177	436	1680
19	2029+0456	20 29 43.40	04 56 11.3	21.7	0.789	28.9	73	153	364
20	2224+0513	22 24 17.89	05 13 47.3	21.3	0.974	36.1	120	328	790
21	2247+0507	22 47 15.18	05 08 09.0	22.1	1.055	5.6	120	347	885
22	2348+0507	23 48 32.01	05 07 33.8	22.8	2.014	4.7	145	399	1151

No.	α_{3940}	α_{500}	L_{3940} WHz^{-1}	L_{500} WHz^{-1}	Morphology	Note
1	11	12	13	14	15	16
1	-1.221	-0.84	8.77×10^{25}	5.96×10^{26}	T,BC,FRII	abs
2	-0.817	-1.031	2.63×10^{26}	1.98×10^{27}	D,FRII	abs
3	-1.154	-1.142	1.66×10^{27}	1.57×10^{28}	CL	n(Lyα)
4	-0.925	-0.925	4.12×10^{26}	3.21×10^{27}	T,C,FRII	abs
5	-1.091	0.789	1.70×10^{26}	1.23×10^{27}	P	BLRG; B + abs
6	-1.366	-1.095	2.38×10^{28}	3.19×10^{29}	T,BC,FRII	n(Lyα)
7	-1.098	-0.911	1.02×10^{27}	8.13×10^{27}	D,FRII	n
8	-0.961	-0.531	1.99×10^{26}	7.24×10^{26}	D,FRII	abs
9	-1.275	-1.095	7.33×10^{26}	1.02×10^{28}	D,FRII	n(Lyα)
10	-0.945	-0.83	7.46×10^{26}	4.39×10^{27}	D, FRII	BLRG
11	-0.927	-0.927	1.26×10^{26}	8.52×10^{26}	P	n
12	-0.977	0.735	9.71×10^{25}	4.93×10^{26}	T,BC,FRII/I	abs
13	-1.1	-0.806	7.74×10^{25}	4.71×10^{26}	D,FRII	n
14	-0.899	-0.899	2.18×10^{26}	1.39×10^{27}	D,FRII	n
15	-1.208	-0.860	1.51×10^{26}	1.04×10^{27}	CJ	BLRG;B+abs
16	-0.728	-0.728	1.54×10^{26}	6.91×10^{26}	D,FRII	n+abs
17	-1.176	-1.047	2.22×10^{27}	1.87×10^{28}	D,FRII	n(Lyα)
18	-0.875	-0.875	9.53×10^{26}	5.82×10^{27}	T,BC,FRII	n
19	-0.78	-0.78	1.34×10^{26}	6.66×10^{26}	T,BC,FRII	n
20	-1.032	-0.796	3.65×10^{26}	2.66×10^{27}	D,FRII	n
21	-0.966	-0.966	4.63×10^{26}	3.40×10^{27}	D,C?,FRII	BLRG

Table 2. Radio galaxies with $z < 0.7$.

No.	RCJ name	RA	Dec	m_R	z_{sp}	LAS	S_{3940} mJy	S_{1400} mJy	S_{500} mJy
1	2	3	4	5	6	7	8	9	10
1	0110+0500	$01^h10^m13.91^s$	04°59'57.6"	21.3	0.633	74.4"	94	247	566
2	0135+0450	01 35 37.20	04 48 33.8	18.4	0.372	7.8	101	255	665
3	0209+0501A	02 09 12.56	05 00 52.2	18.5	0.285	0.4	33.4	86	242
4	0457+0452	04 57 53.86	04 53 53.5	19.4	0.482	67	72	199	461
5	0820+0454	08 20 56.7	04 54 16.8	19.3	0.539	2.0	165	465	1206
6	0845+0444	08 45 31.20	04 42 54.9	21.4	0.650	7.6	156	504	1164
7	0908+0451	09 08 21.01	04 50 58.3	19.6	0.525	34.5	111	263	700
8	1011+0502	10 12 04.58	05 06 14.2	22.4	0.456	1.3	68	210	545
9	1124+0456	11 24 37.43	04 56 18.7	17.3	0.284	12.0	440	991	2716
10	1142+0455	11 42 20.10	04 54 56.0	21.0	0.605	18.7	107	292	652
11	1155+0444	11 55 19.24	04 43 31.3	18.6	0.289	13.0	71	159	353
12	1235+0435	12 35 49.52	04 32 56.9	21.5	0.657	9.1	61	153	300
13	1446+0507	14 46 17.97	05 07 41.1	19.3	0.273	68.0	163	364	746
14	1646+0501	16 46 53.31	05 01 10.0	21.2	0.690	15.7	55	106	313
15	1722+0442	17 22 14.06	04 43 17.0	20.7	0.604	21.9	266	768	2049

No.	α_{3940}	α_{500}	L_{3940} WHz^{-1}	L_{500} WHz^{-1}	Morphology	Note
1	11	12	13	14	15	16
1	-0.994	-0.744	1.20×10^{26}	6.46×10^{26}	D,FRII	n+abs
2	-0.955	-0.88	4.02×10^{25}	2.53×10^{26}	TB,C,FRII	n+abs
3	-0.96	-0.96	8.20×10^{24}	4.53×10^{25}	P	abs
4	-1.059	-0.731	5.27×10^{25}	2.97×10^{26}	D,FRII/I	n+abs
5	-0.993	-0.993	1.50×10^{26}	1.09×10^{27}	D,FRII	n
6	-1.19	-0.753	2.34×10^{26}	1.34×10^{27}	T,C,FRII	n+abs
7	-0.944	-0.845	9.28×10^{25}	5.64×10^{26}	T,C,FRII	BLRG;B+abs
8	-1.01	-1.01	4.34×10^{25}	3.47×10^{26}	CL	n
9	-0.914	-0.849	1.00×10^{26}	6.18×10^{26}	D,FRII	n+abs
10	-0.874	-0.874	1.18×10^{26}	7.16×10^{26}	T,C,FRII	n+abs
11	-0.778	-0.778	1.61×10^{25}	8.05×10^{25}	D,FRII	n+abs
12	-0.822	-0.720	7.80×10^{25}	3.64×10^{26}	D,FRII	abs
13	-0.736	-0.736	3.27×10^{25}	1.50×10^{26}	T,WC,FRII	n+ab
14	-0.84	-0.84	7.85×10^{25}	4.47×10^{26}	D,FRII	abs
15	-1.061	-0.918	3.18×10^{26}	2.29×10^{27}	D,FRII	n+abs

Table 3. Quasars.

No.	RCJ name	RA	Dec	m_R	z_{sp}	LAS	S_{3940} mJy	S_{1400} mJy	S_{500} mJy
1	2	3	4	5	6	7	8	9	10
1	0038+0449	$00^h38^m34.65^s$	04°50'50.5"	2.446	3.3'	21.2	94	239	640
2	0042+0504	00 42 27.14	05 05 24.1	1.504	24.8	19.0	93	231	579
3	0126+0502	01 26 16.13	05 02 10.3	1.008	18.0	18.1	51	151	402
4	0143+0505	01 43 33.97	05 07 58.0	2.135	7.4	20.6	52	164	485
5	0226+0512	02 26 19.81	04 46 32.3	1.235	10.7	20.1	98	242	532
6	0459+0456	04 59 04.28	04 55 54.4	1.189	63.8	20.9	90	251	564
7	1100+0444	11 00 11.49	04 44 01.4	0.890	0.3	19.1	239	640	1453
8	1154+0431	11 54 53.50	04 24 12.5	0.998	6.7	19.9	331	854	1867
9	1251+0446	12 51 29.50	04 46 41.7	0.96	257	19.3	204	514	1611
10	1333+0451	13 33 07.00	04 50 48.6	1.405	129.5	17.3	21	55	123
11	1456+0456	14 56 25.79	04 56 44.8	2.13	2.2	20.0	110	288	727
12	1740+0502	17 40 33.96	05 02 42.3	3.57	4.7	22.6	36	110	288
13	2013+0508	20 13 23.48	05 10 30.5	0.89	10.0	21.1	53	138	281
14	2036+0451	20 36 56.93	04 49 52.7	0.716	56.0	19.0	80	228	563
15	2144+0513	21 44 27.18	05 11 15.2	1.01	1.9	18.8	66	203	526
16	2225+0523	22 25 14.72	05 27 09.1	2.323	2.7	17.8	309	849	2219
17	2320+0459	23 20 44.74	04 59 24.9	1.39	15.2	20.4	78	169	423

No.	α_{3940}	α_{500}	L_{3940} WHz^{-1}	L_{500} WHz^{-1}	Morphology	Note
1	11	12	13	14	15	16
1	-1.08	-0.776	2.68×10^{27}	1.25×10^{28}	FRII D.	B(Lyα)
2	-0.937	-0.836	7.61×10^{26}	4.32×10^{27}	D, FRII	B
3	-1.133	-0.874	1.99×10^{26}	1.31×10^{27}	D, FRII	B
4	-1.245	-0.926	1.31×10^{27}	8.47×10^{27}	D, FRII	B(Lyα)
5	-0.947	-0.686	5.33×10^{26}	2.34×10^{27}	D, FRII	B
6	-1.167	-0.615	5.27×10^{26}	2.14×10^{27}	D, FRII	B
7	-0.874	-0.874	5.98×10^{26}	3.63×10^{27}	P	B
8	-0.994	-0.682	1.15×10^{27}	5.22×10^{27}	D, FRII	B
9	-1.129	-0.875	7.12×10^{26}	4.74×10^{27}	D, FRII	B
10	-1.09	-0.702	1.69×10^{26}	7.07×10^{26}	T,C,FRII	B
11	-0.875	-0.875	1.80×10^{27}	1.19×10^{28}	D?	B
12	-1.148	-0.870	2.71×10^{27}	1.43×10^{28}	CL	B (Lyα)
13	-0.809	-0.809	1.27×10^{26}	6.74×10^{26}	D, FRII	B
14	-1.076	-0.816	1.40×10^{26}	8.58×10^{26}	T,C,FRII	B
15	-1.066	-1.066	2.47×10^{26}	1.97×10^{27}	T,C,FRII	B
16	-0.995	-0.902	7.04×10^{27}	4.50×10^{28}	T,C,FRII	B
17	-0.868	-0.769	5.05×10^{26}	2.52×10^{27}	D, FRII	B

Table 4. Radio galaxies with no emission lines detected.

No.	RCJ name	RA	Dec	m_R	LAS	S_{3940} mJy
1	2	3	4	5	6	7
1	0015+0503a	00 15 11.61	05 06 39.8	22.0	20.6	19
2	0250+0512	02 50 53.57	05 16 12.7	>24.5	1.2	68
3	0308+0454	03 08 33.95	04 54 10.3	23.3	1.2	29
4	0324+0442	03 24 07.32	04 42 01.8	22.4	11.8	120
5	0355+0449	03 55 12.72	04 40 41	24.2	2.4	62
6	0446+0525	04 46 23.17	05 40 50.2	23.2	19.17	107
7	0743+0455	07 43 15.59	04 55 52.5	23.6	20.5	37
8	0836+0511	08 36 48.09	05 13 09.0	22.6	19.6	113
9	0945+0454	09 45 26.81	04 54 13.7	23.5	4.5	20
10	1051+0449	10 51 25.78	04 49 43.9	22.5	1.7	122
11	1148+0455	11 48 47.88	04 55 24.4	23.2	43.9	250
12	1152+0449	11 52 23.67	04 48 14.3	22.5	7.0	46
13	1703+0502	17 03 29.32	05 02 11.6	23.5	1.8	210
14	1720+0455	17 20 04.6	04 53 48.8	(20.6)	¡0.5	19
15	1735+0454	17 35 41.76	04 55 15.3	23.2	5.2	28
16	2219+0458	22 19 06.13	04 58 45.7	23.8	4.7	50
17	2236+0454	22 36 51.17	04 55 09.2	23.6	40.2	41

No.	α_{3940}	α_{500}	Morphology	Exposure time and note
1	8	9	10	11
1	-1.67	-1.03	D, FRII	2×900s
2	-1.26	-1.26	D, FRII	4×900s
3	-0.965	-0.965	CL or D, BC,FRII	4×900s,3×1200s,6×900s
4	-1.131	-0.974	D, FRII/I	6×900s,4×900s
5	-1.494	-1.296	D, FRII	2×900s,4×900s
6	-0.983	-0.983	D, FRII	3×900s
7	-1.064	-1.064	D, FRII	2×900s
8	-1.05	-1.05	D, CJ, FRII/I	4×120s
9	-1.01	-1.01	D, FRII	4×900s
10	-0.92	-0.92	D, FRII	2×900s
11	-1.24	-0.94	D, FRII	2×900s
12	-0.762	-0.762	D, FRII	3×900s
13	-1.05	-1.05	D, FRII	3×900s, 2×600,900s, 2×900s
14	-1.01	-1.41	P	600s; M star by spectrum
15	-0.924	-0.924	D, FRII	4×900s
16	-1.227	-0.861	D, FRII	2×900s
17	-1.517	-0.899	D, FRII	2×900s, 4×1200s

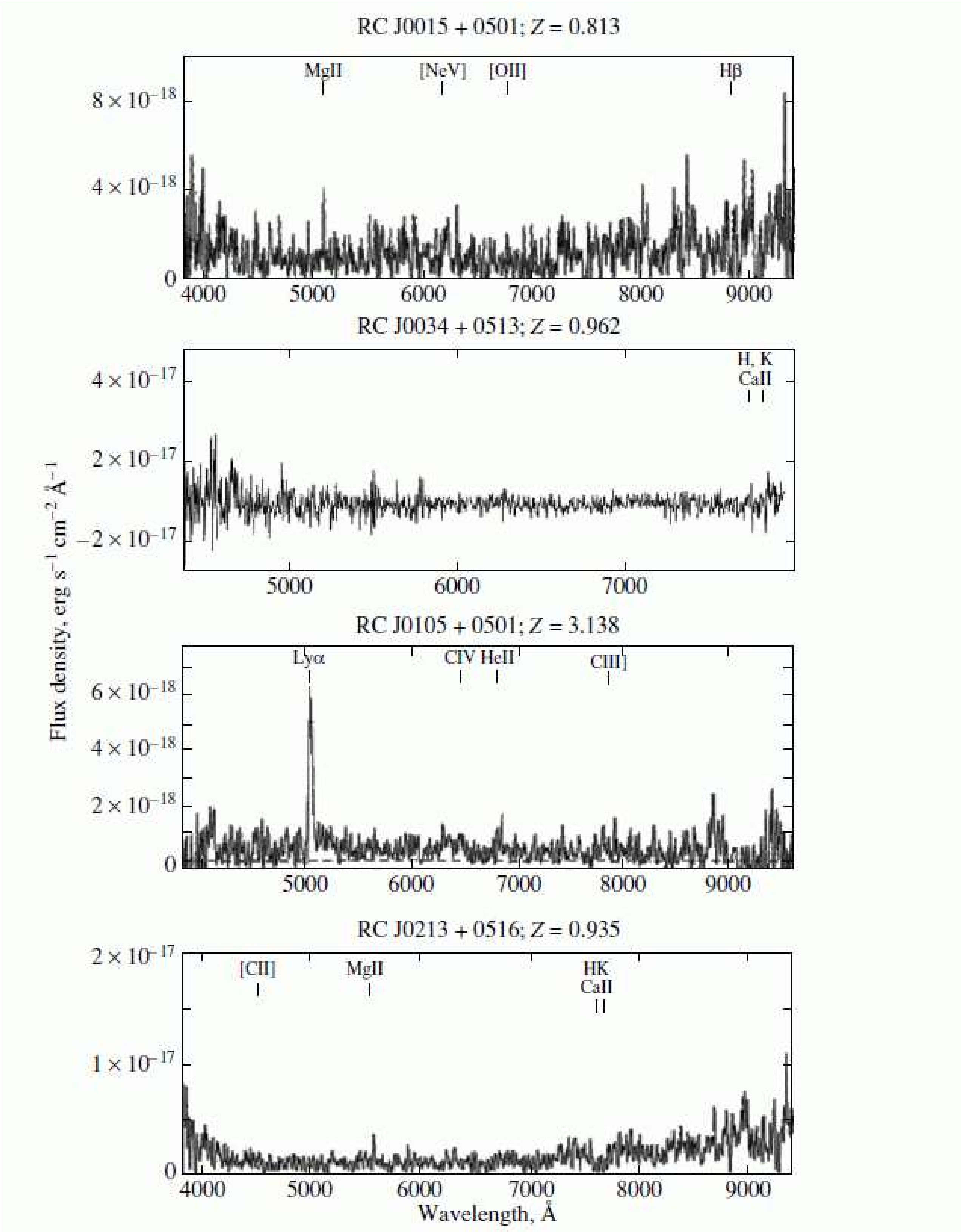

Figure 1: Spectra of radio galaxies with $z > 0.7$.

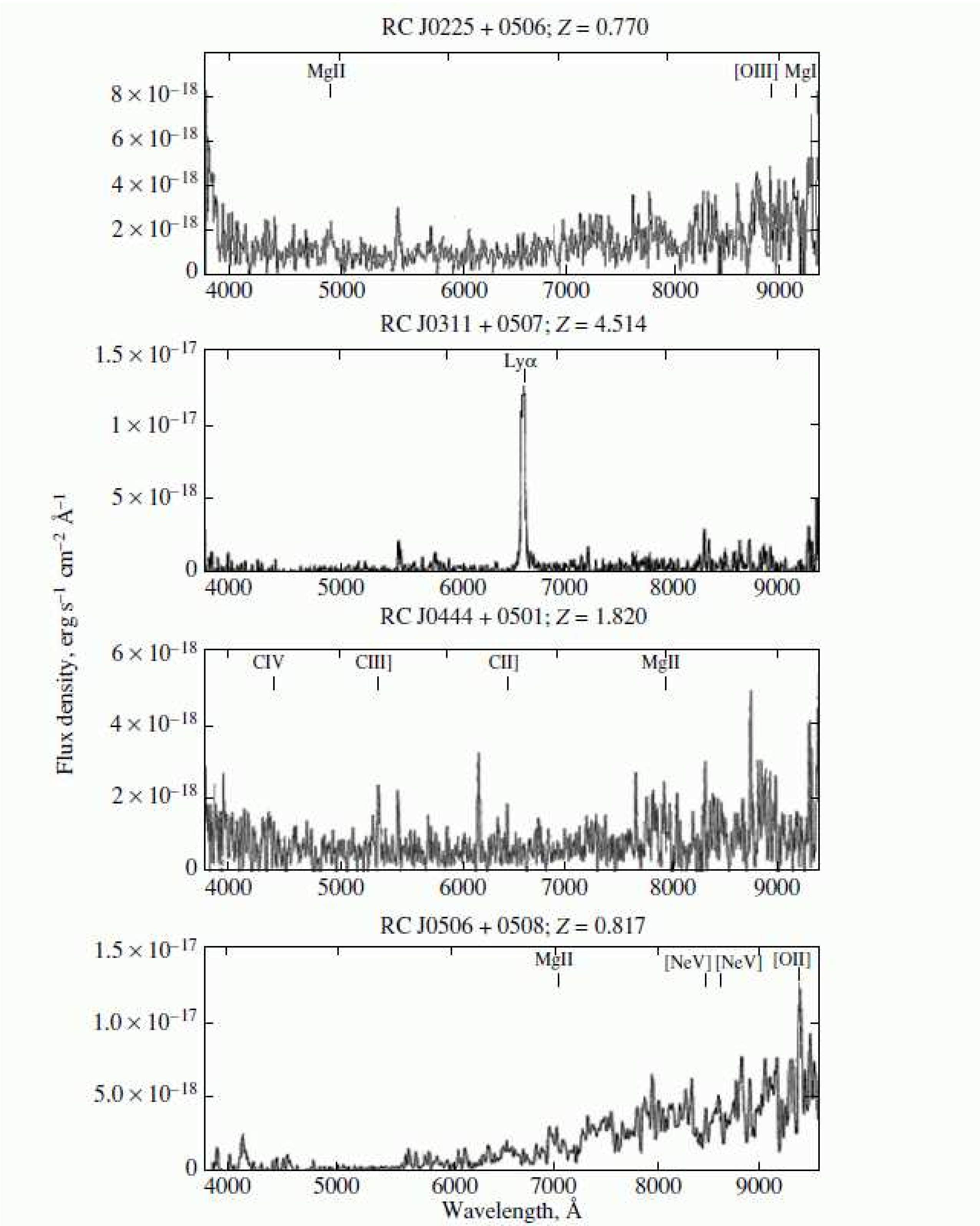

Fig. 1. (Continued)

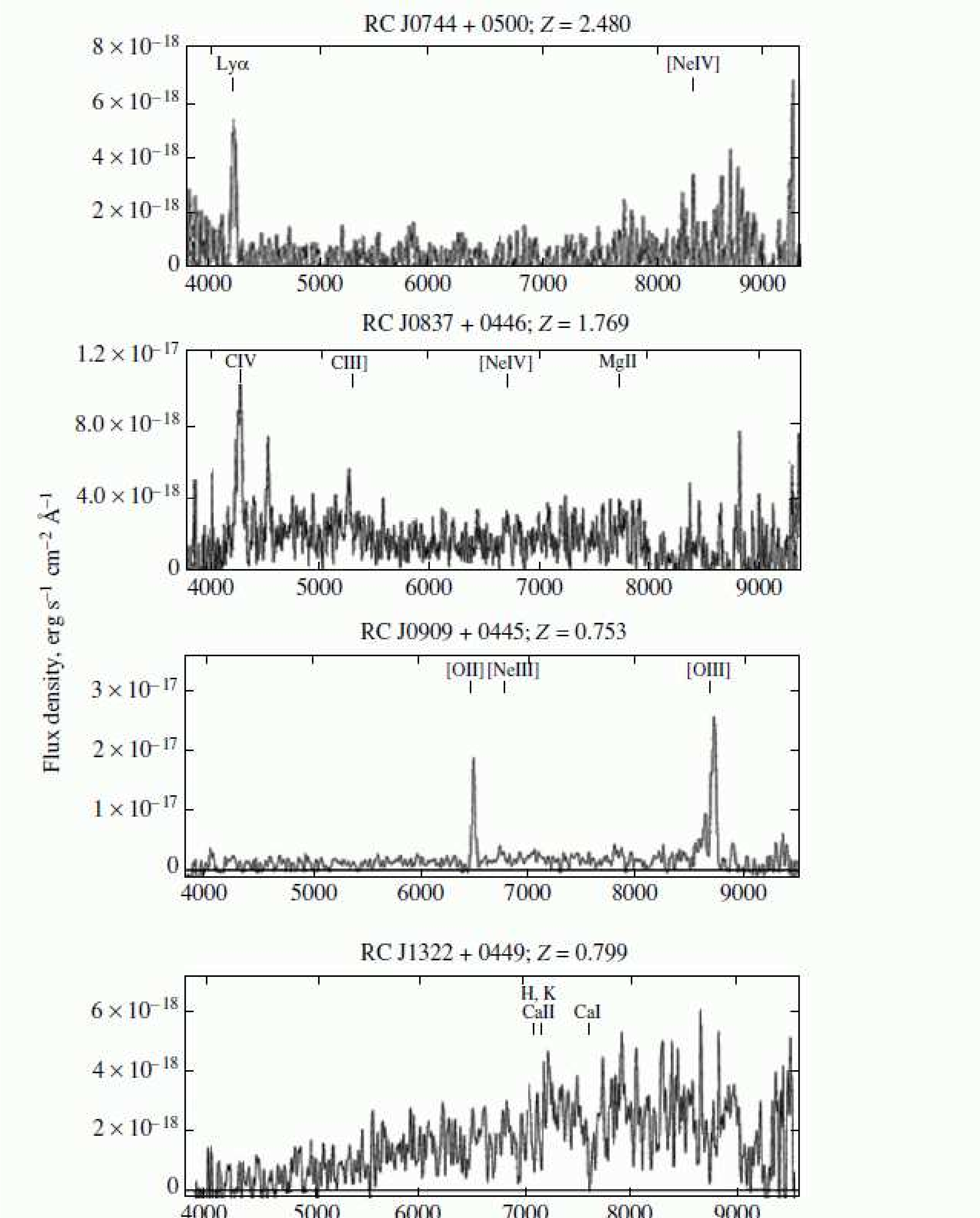

Fig. 1. (Continued)

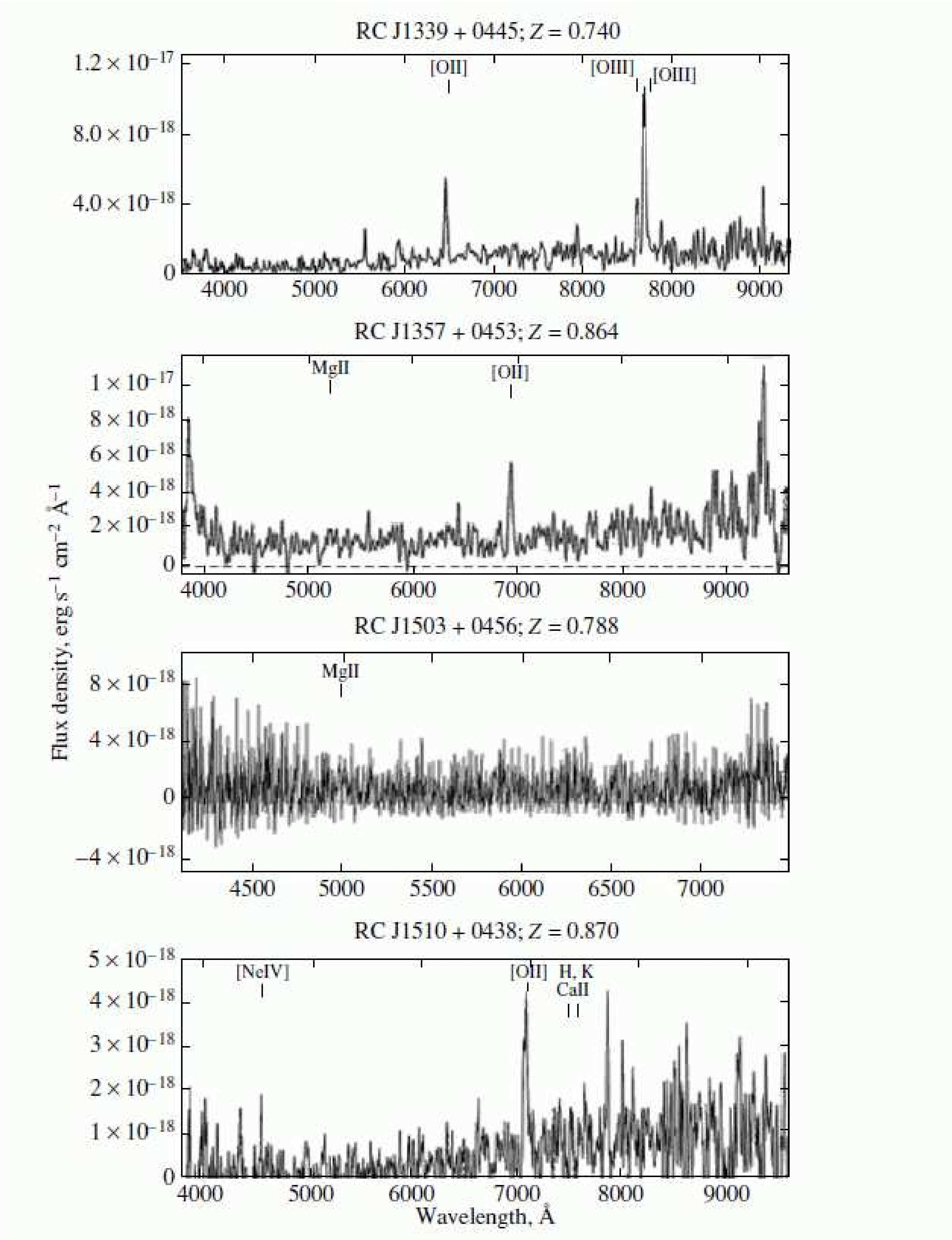

Fig. 1. (Continued)

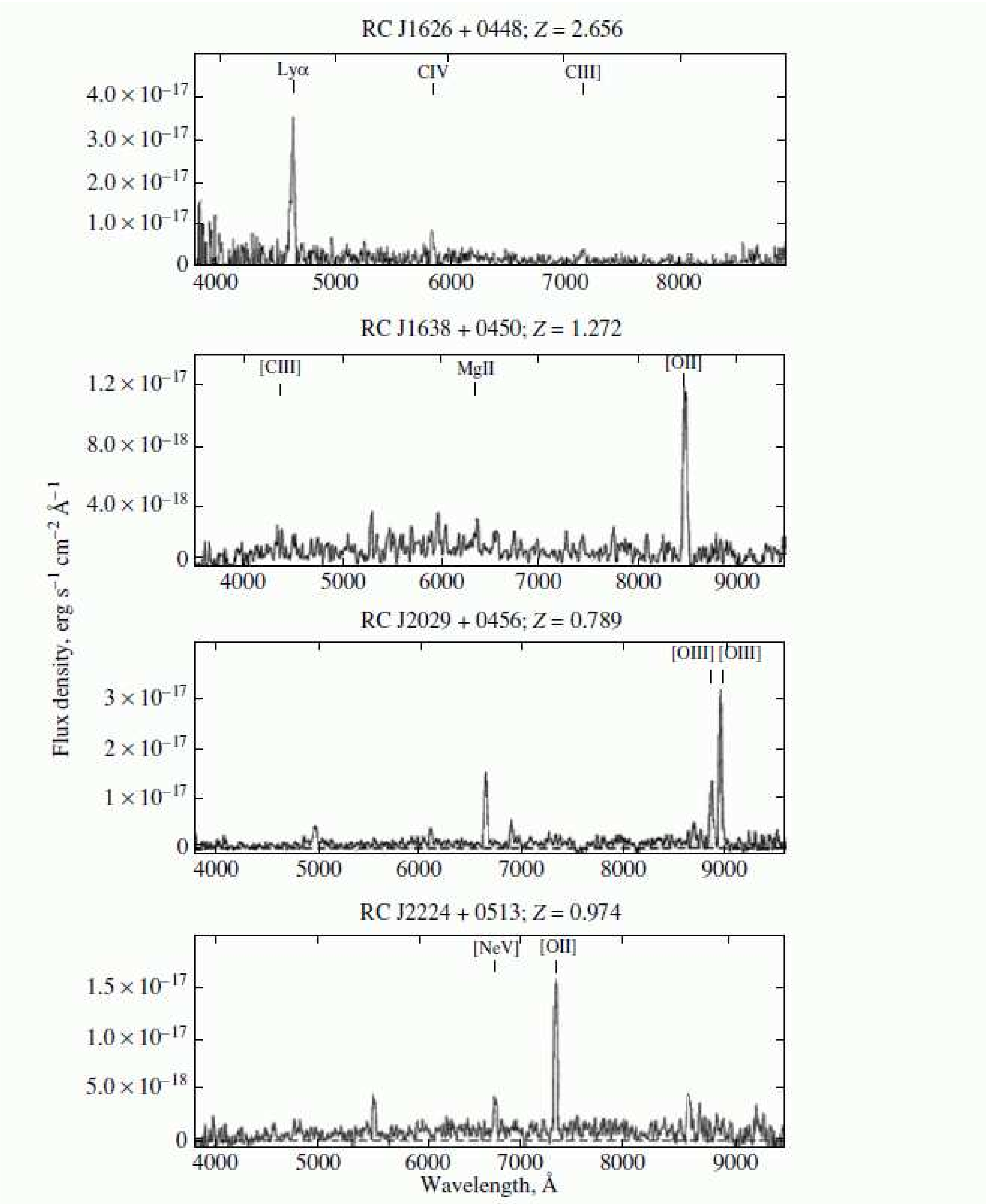

Fig. 1. (Continued)

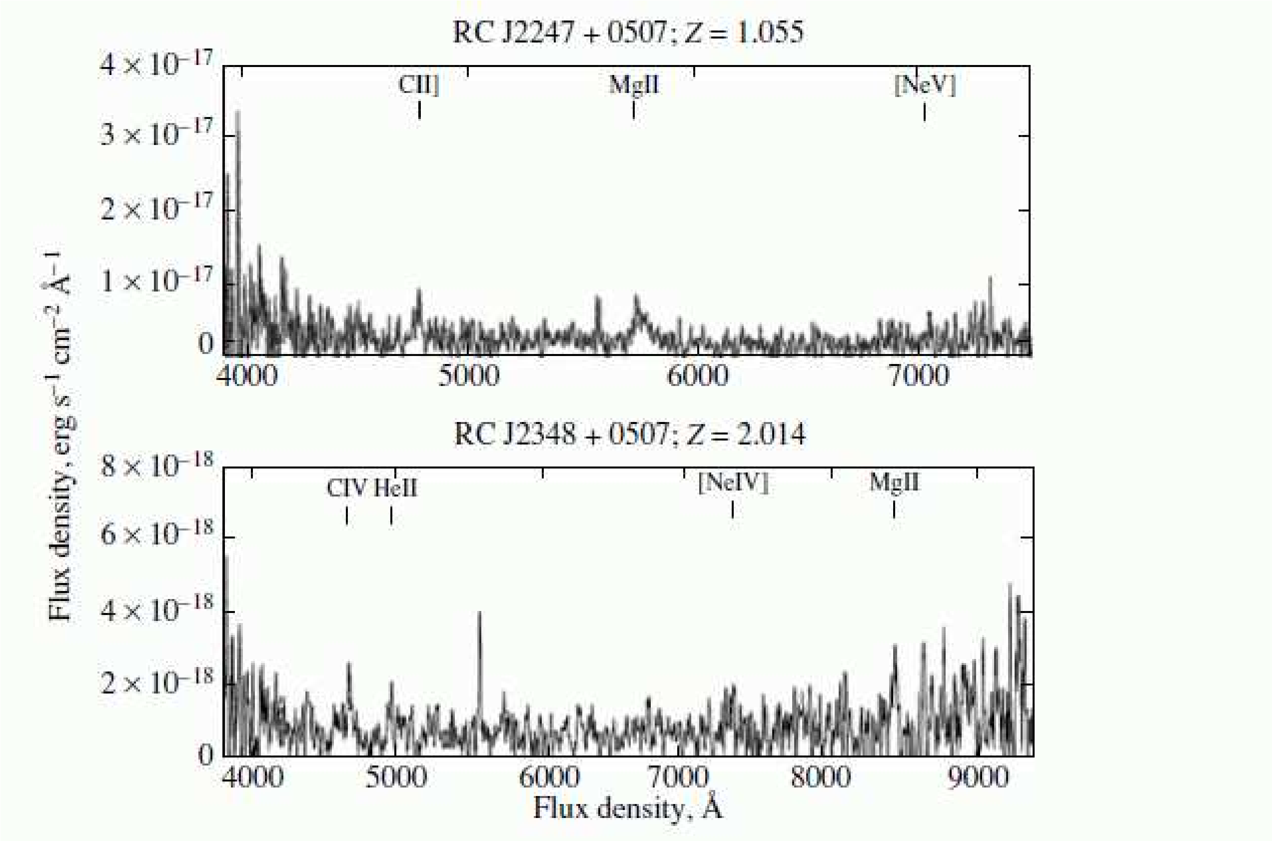

Fig. 1. (Continued)

source, 'T' a triple source, 'C' the presence of a core, 'BC' the presence of a bright core, 'WC' the presence of a weak core, 'CL' a core and lobe structure (distinct components), 'CJ' a core and jet structure (the core not distinguishable from the extended jet), and FRI/FRII an object of Fanaroff–Riley types I/II; 16 — notes, with n, B and abs indicating the presence of narrow emission lines, broad emission lines, and absorption lines in the spectrum and BLRG indicating a broad-line radio galaxy.

The columns of Table 3 contain the same information as in Tables 1 and 2 for the 17 detected quasars. Table 4 presents the results for the 17 radio galaxies without detected emission lines.

Columns 1–5 of Table 4 are analogous to the corresponding columns in Tables 1–3. The following columns contain: 6 — the largest angular size in arcseconds, LAS; 7 — the flux density, S, in mJy at 3940 MHz; 8, 9 — the spectral indices α at 3940 and 500 MHz; 10 — the morphology; 11 — the exposure time, in seconds, and notes. Note that the absence of detectable lines for faint objects could, in some cases, be due to a higher redshift (z¿5) or absorption by dust, or bad weather conditions (with seeing ∼2"–3"). One can not also exclude an incorrectly placed spectrograph slit. For example, such objects in Table 4 include RCJ 0250+512 and RCJ 0355+0449, whose spectral indices, morphologies, angular sizes, and ratios of the radio to optical luminosity suggest they may be very distant objects. It would be desirable to obtain spectroscopy of these objects using telescopes with higher sensitivities and broader frequency ranges, repeat the 6-m SAO observations under very good seeing conditions, or obtain observations in the K-filter.

Below we present remarks for several of the radio sources.

RCJ 0015+0503a (Table 4). This object has B=23.98, V=23.04, R=22.26, I=21.40. The observing conditions were poor, with seeing of ∼3"; z_{ph}=0.60±0.13.

RCJ 0034+0513 (Table 1). The redshift was measured from two absorption lines, at 7700 å(the KCaII 3933.7 åline) and 7800 å(the HCaII 3968.5 åline); z_{ph}=1.03.

RCJ 0105+0501 (Table 1). The radio source is double; it is not clear where the AGN is located. An optical object displaying Lyα emission has the coordinates α=01h05m34.091s, δ=+5°01'12.47" (J2000), not coincident with any of the radio components. Radio observations with higher sensitivity and resolution are desirable, in order to detect the radio core. The object's has B=24.1, V=22.5, R=22.8, I=22.4.

RCJ 0213+0516 (Table 1). The object is a cluster member. The brightest member of the cluster is a radio quasar at redshift $z_{sp} = 0.94$ (approximately the same z as for the FRII radio galaxy), 8" to the east of the radio core. The contribution from the compact core is about 3% of the total flux density of the radio source. There is a small jet directed away from the quasar. Interaction between the quasar and the host galaxy cannot be ruled out. (The VLA radio image with overlaid 6-m SAO optical image can be found at `http://wo.sao.ru/hd/zhe`; similar information is also available for other objects at this same address.)

RCJ 0311+0507 (Table 1). This object has the highest redshift in our sample [26, 27]. It has B>24.9, V>24.8, R=22.6, I=22.3. This radio source has now been studied using the "Merlin" radio interferometer (UK) and European VLBI Network (EVN).

RCJ 0324+0442 (Table 4). This is an FRII double radio source, most probably in an empty field (the two galaxies near the eastern component are foreground objects); m_R>25. If such objects are detected in the K-band at the level K=18–19, they enter the range z_{sp}=1.5–2, and have no bright emission lines in the optical.

RCJ 0506+0508 (Table 1). The redshift was determined from absorption lines at 7150–7250 å(though there remain some doubts).

RCJ 0836+0511 (Table 4). This is not an entirely classical FRII object: the radio map at 8460 MHz (VLA) reveals a core, a jet toward the Northeast, a hot spot, and a "tail"; z_{ph}=1.12.

RCJ 0908+0451 (Table 2). z_{sp}=0.542, based on data from the NASA Extragalactic Database (NED).

RCJ 1011+0502 (Table 2). This is the faintest galaxy among the RC objects, with the lowest luminosity in the optical (possibly a Sy1 galaxy with a strong jet).

RCJ 1051+0449 (Table 4). The direct images give B=23.77, V=23.12, R=22.74, while the object was not detected in the I-band (the images were taken in the presence of seeing of 1.5"); no images of a BVRI standard were taken, and the reduction was made using surrounding SDSS objects.

RCJ 1100+0444 (Table 3). The NED-based redshift is z_{sp}=0.8861.

RCJ 1124+0456 (Table 2). The NED-based redshift is z_{sp}=0.2827.

RCJ 1148+0455 (Table 4). The NED redshift, z_{sp}=0.42,is not confirmed.

RCJ 1152+0442 (Table 4). The photometric redshift z_{ph}=1.24, disagrees with our results.

RCJ 1333+0451 (Table 3). The NED-based redshift is z_{sp}=1.4024; z_{ph}=1.07.

RCJ 1503+0456 (Table 1). It is more likely that the broad emission line at 5002 åis MgII 2798 åthan CIII] 1909 å. The MgII identification is favored, with a possibly detected continuum jump redward of 7150 å(z_{sp}=0.788). This is a BLRG, consistent with its magnitude and radio morphology (core+jet); z_{ph}=0.88.

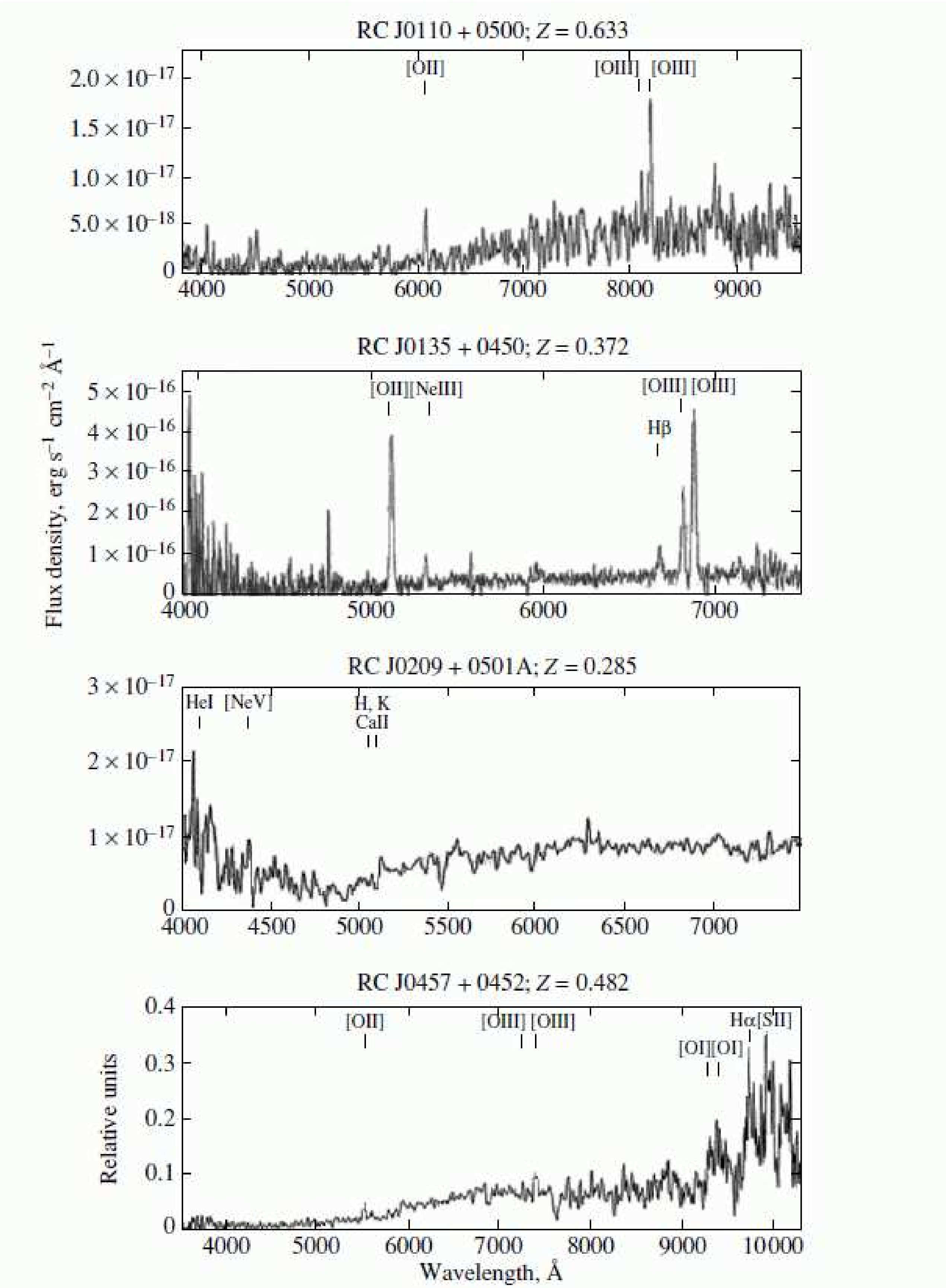

Figure 2: Spectra of radio galaxies with z¡0.7.

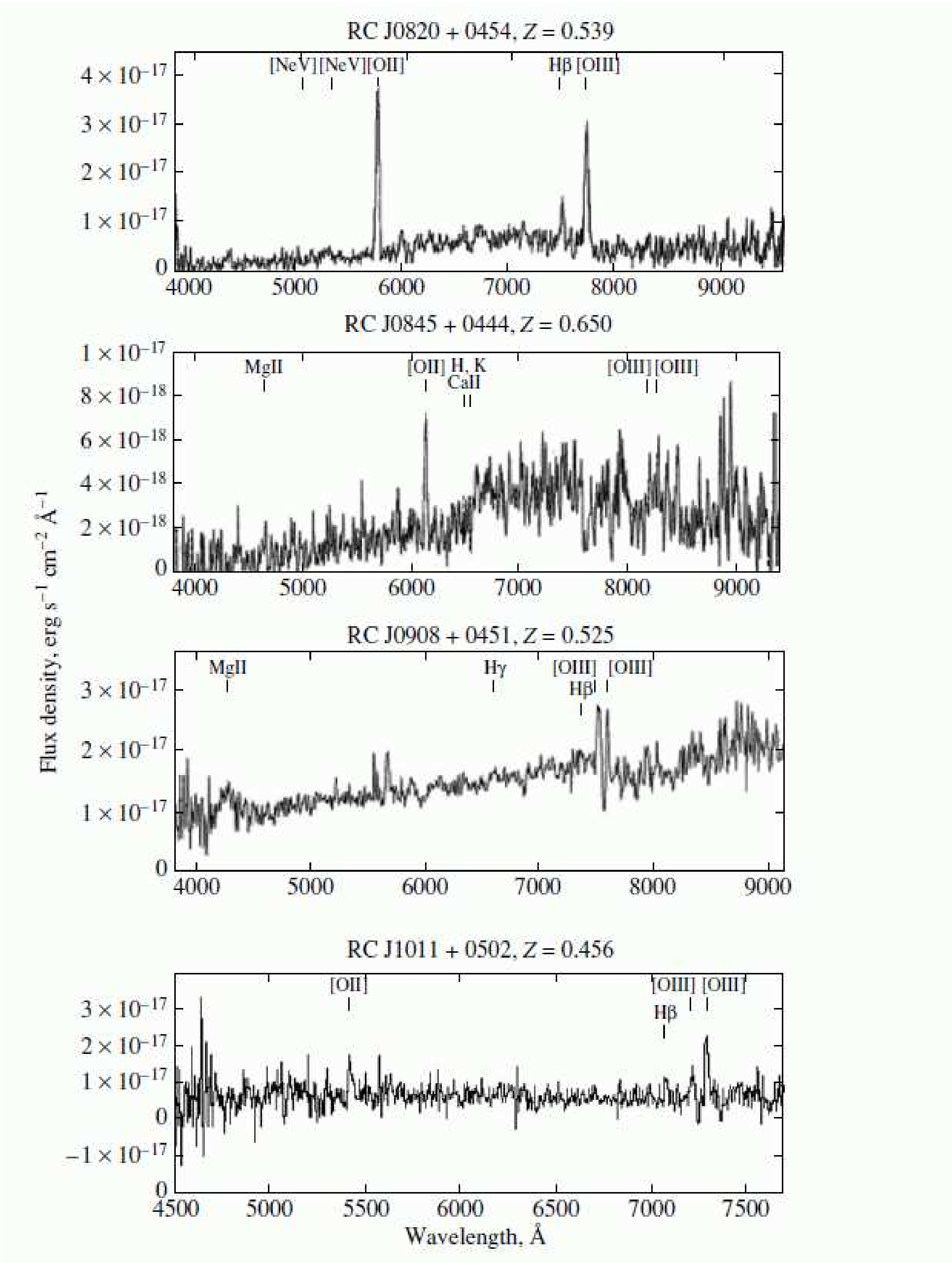

Fig. 2. (Continued)

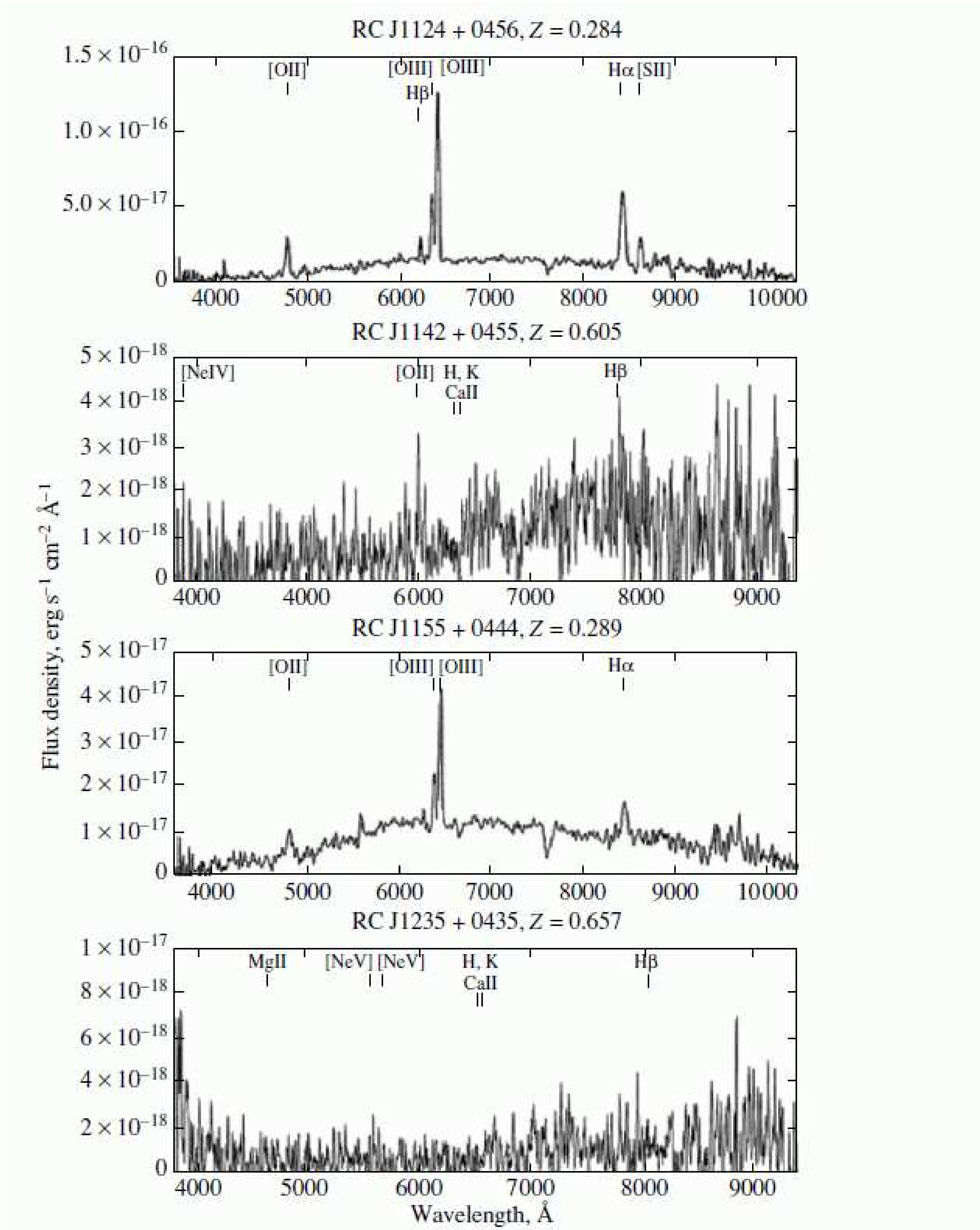

Fig. 2. (Continued)

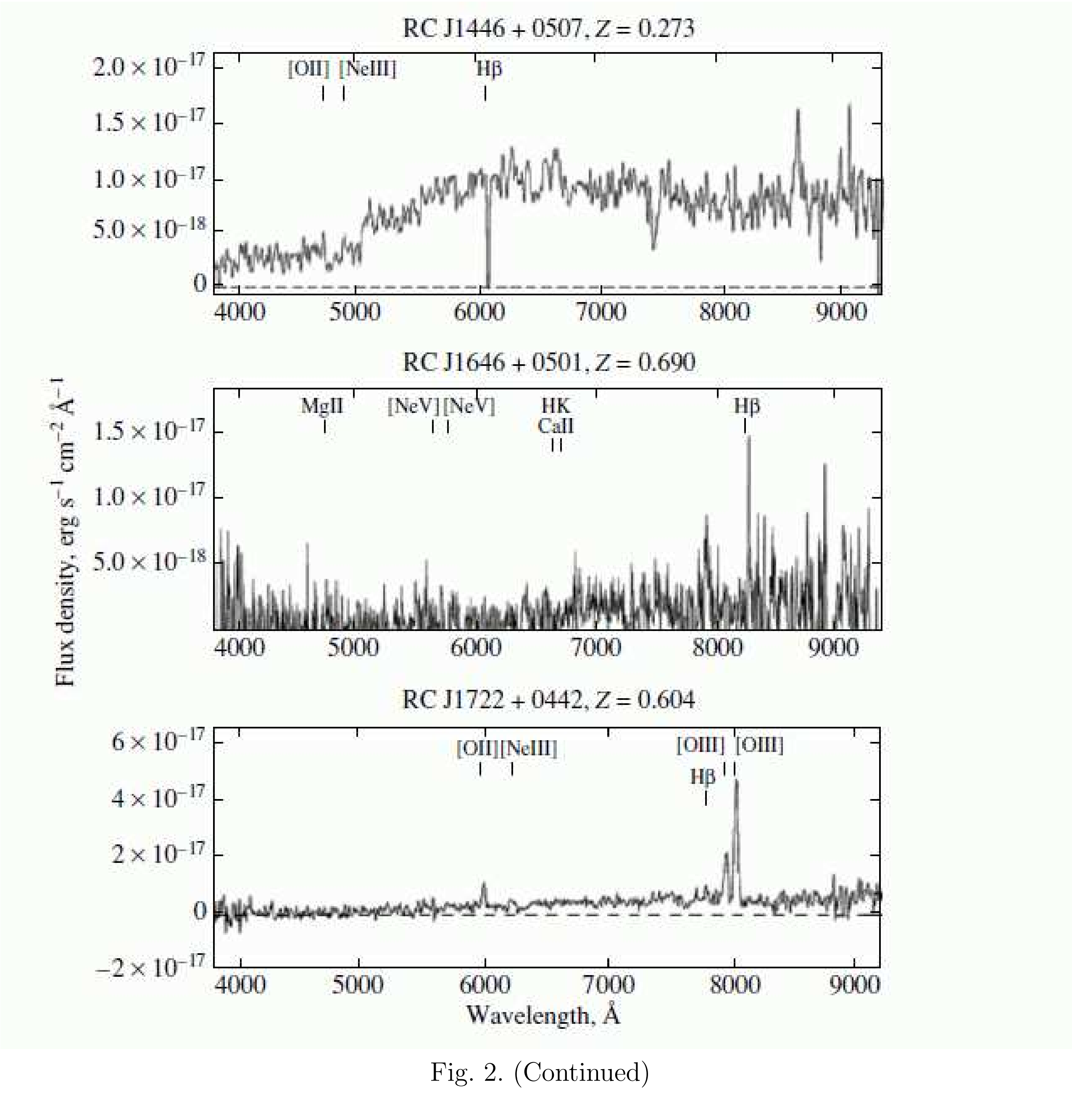

Fig. 2. (Continued)

RCJ 1735+0454 (Table 4). No continuum or bright emission lines were detected. If the weak emission at 7274 åis [OII] 3727 å, then the redshift is z_{sp}=0.952. However, the spectrum to the red is too short to see the continuum jump and confirm this hypothesis.

RCJ 1740+0502 (Table 3). This object has a broad Lyα line (5560 å) but no CIV line. This is a star-like object in the optical, i.e., with a dominant nucleus. However, it is not a typical quasar; such objects are sometimes called WQs (weak quasars).

RCJ 2219+0458 (Table 4). The continuum grows to the blue, in contradiction with the galaxy's colors (B=24.8, V=25.03, R=23.72, I=22.25); $z_{ph} = 1.24$.

RCJ 2225+0523 (Table 3). The NED-based redshift is $z_{sp} = 2.323$.

RCJ 2247+0507 (Table 1). The spectrum contains a single broad emission line, MgII 2798 å.

The optical spectra of radio galaxies with $z > 0.7$ and $z < 0.7$ are shown in Figs. 1 and 2. Figure 3 displays the spectra of the quasars.

Thus, among the 22 radio galaxies in Table 1, we detected one object with $z = 4.51$, one with $3 \leq z < 4$ $z < 4$,three with $2 \leq z < 3$, and four with $1 \leq z < 2$. Three more objects have redshifts close to unity (>0.9). The redshifts of 10 sources are in the range from 0.74 to 0.87. The redshifts of the 15 radio galaxies from Table 2 are between 0.27 and 0.69. Note that there are no objects with LAS>12" among the nine radio galaxies with $z > 1$.The 500-MHz spectral indices of the objects with $z > 1$ are the same as or lower than their spectral indices at 3940 MHz. As a rule, the spectral indices of such objects at 3940 MHz exceed unity. Two of the three objects with $z > 3$ (RCJ 0105+0501 and RCJ 1740+0502) have CL (core and lobe) structure, while the third object (RCJ 0311+0507) is a strongly asymmetric triple, almost a CL source.

One object among the 17 quasars has z=3.57 (RCJ 1740+0502), four have $2 \leq z < 3$, seven have $1 \leq z < 2$, four have $0.89 \leq z < 1$, and onehas z=0.72.

Figures 4 and 5 display the redshift distributions of the radio galaxies and quasars.

3. CONCLUSIONS

The "Big Trio" project includes about 100 objects, for 71 of which we have obtained optical spectra with the "Scorpio" spectrograph mounted on the 6-m telescope of the SAO (17 quasars and 54 radio galaxies).

Of the studied radio galaxies, four have redshifts $1 \leq z < 2$, three have $2 \leq z < 3$, one has $3 \leq z < 4$, and one has z=4.51. Thirteen sources have $0.7 < z < 1$ and 15 have $0. < z < 0.7$. Five of the program quasars have $0.7 < z < 1$, seven have $1 \leq z < 2$, four have $2 < z < 3$,and one has $z = 3.57$. We detected no spectral lines for 17 objects.

Among the studied steep-and ultra-steep spectrum radio sources with measured redshifts z (54 objects), we found ∼39to have $z > 2$, ∼6% to have $z > 3$, and ∼2% to have $z > 4.5$ (4.514). The total number of radio galaxies with redshifts $z > 4$ detected to date is currently six [28].

The failure to detect spectral lines in the spectra of 17 radio galaxies may indicate that they have redshifts in the range of $1.5 < z < 2$ or $z > 5$, or may be due to absorption by dust. In some cases, observational errors or poor weather conditions could also be responsible.

Our data confirm the effectiveness of identifying candidate distant objects based on the properties of their radio and optical continua (steep radio spectra, characteristics of FRII objects, small angular sizes, large ratios of the radio and optical luminosities). These criteria

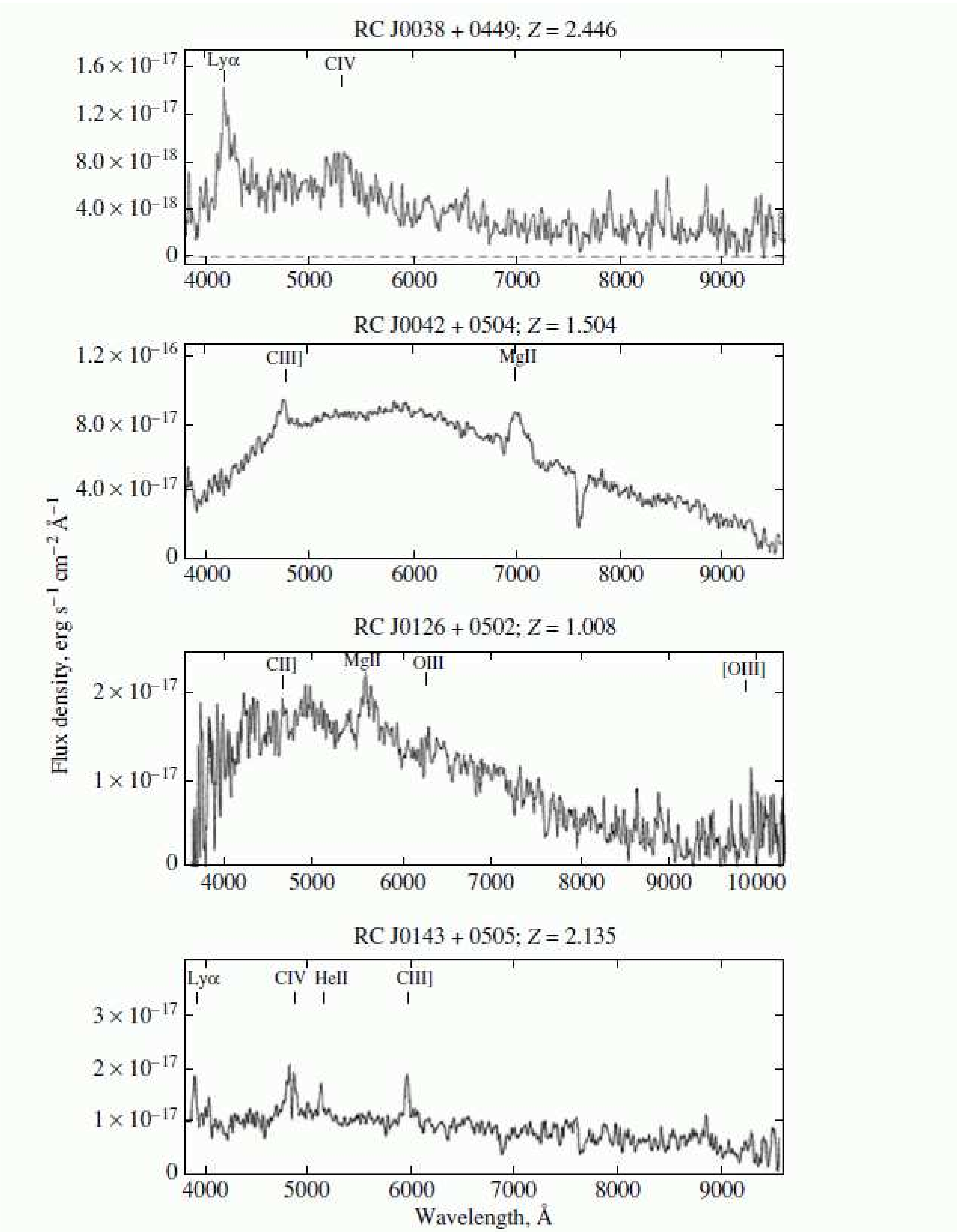

Figure 3: Spectra of quasars.

Fig. 3. (Continued)

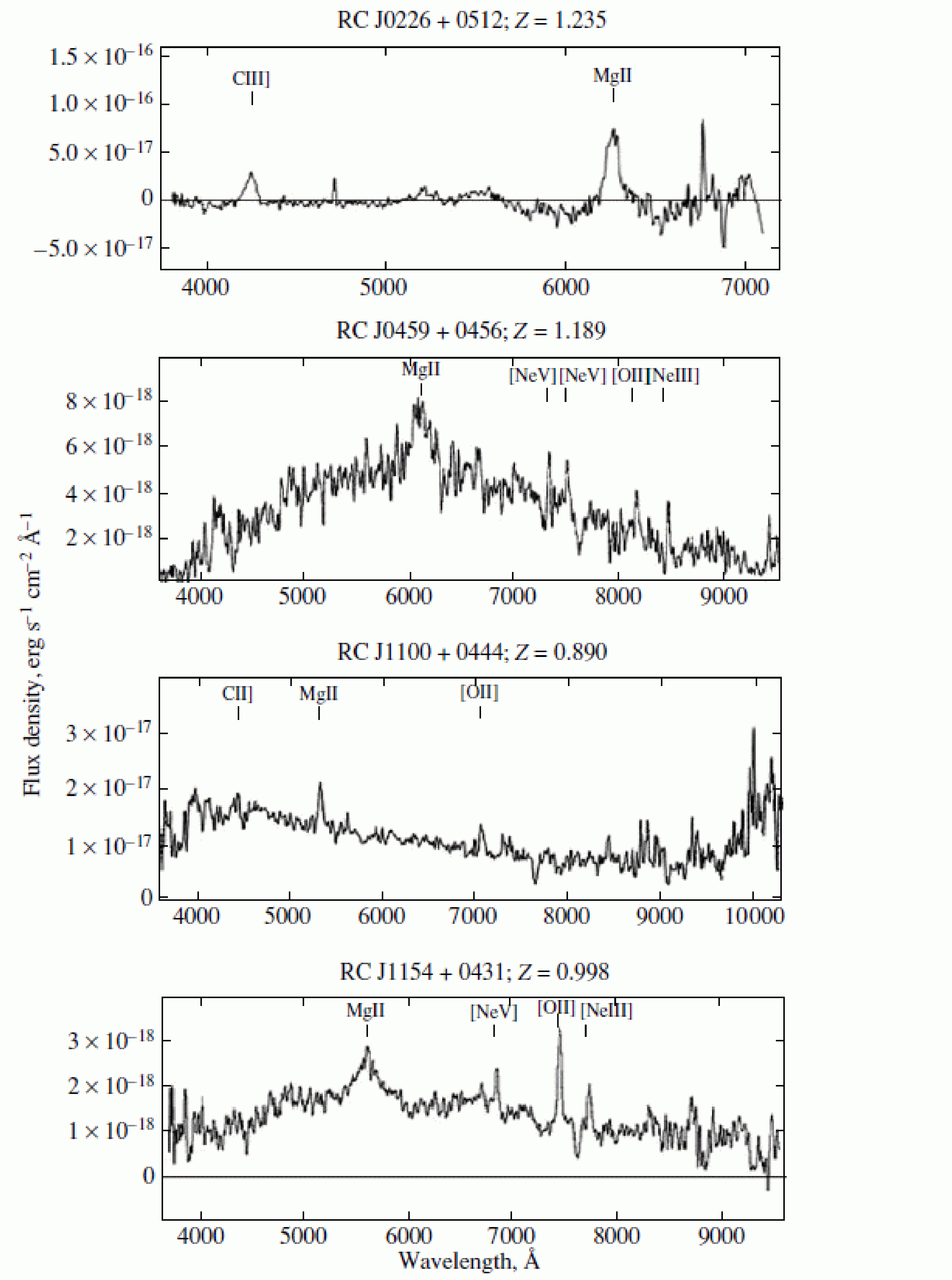

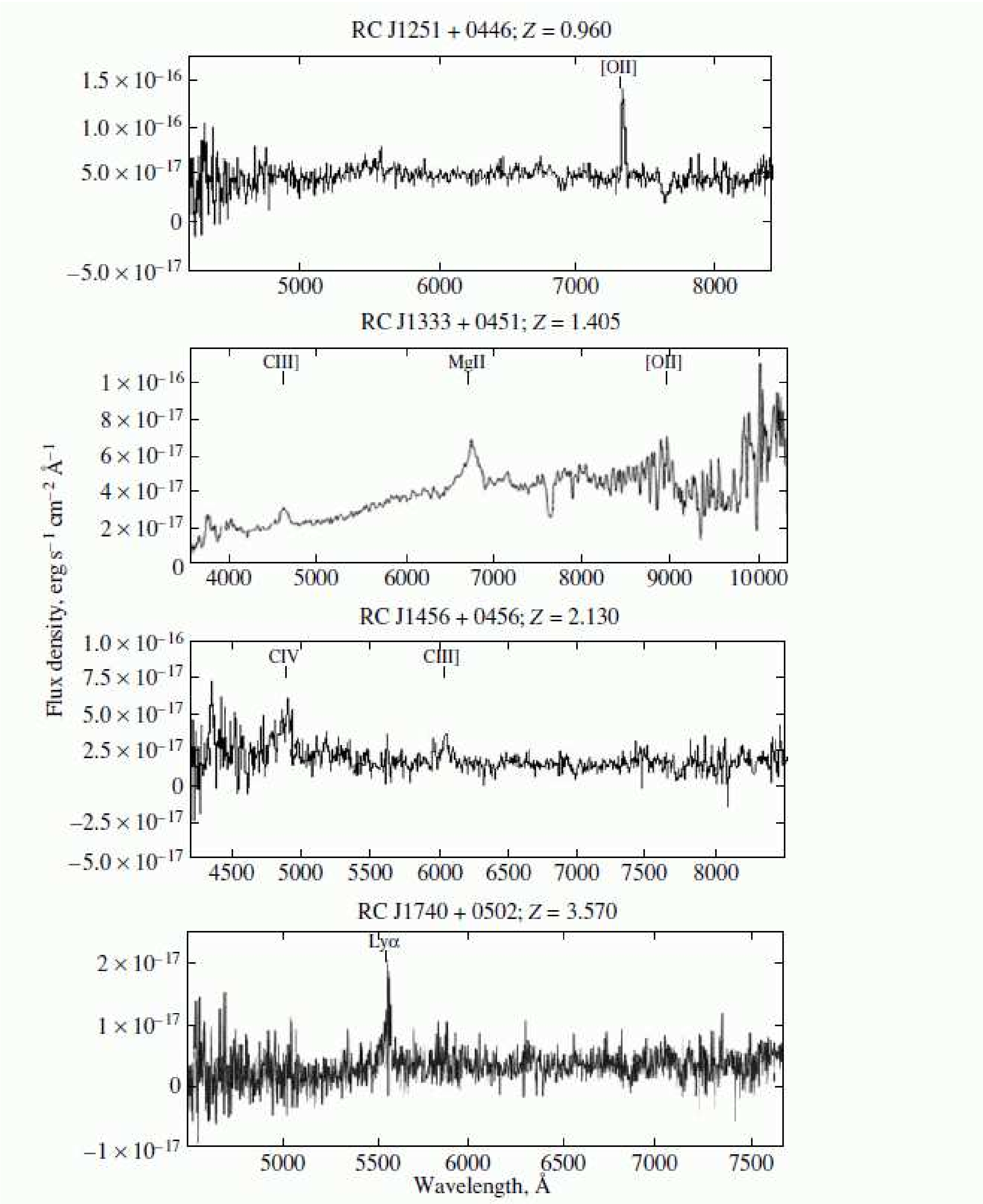

Fig. 3. (Continued)

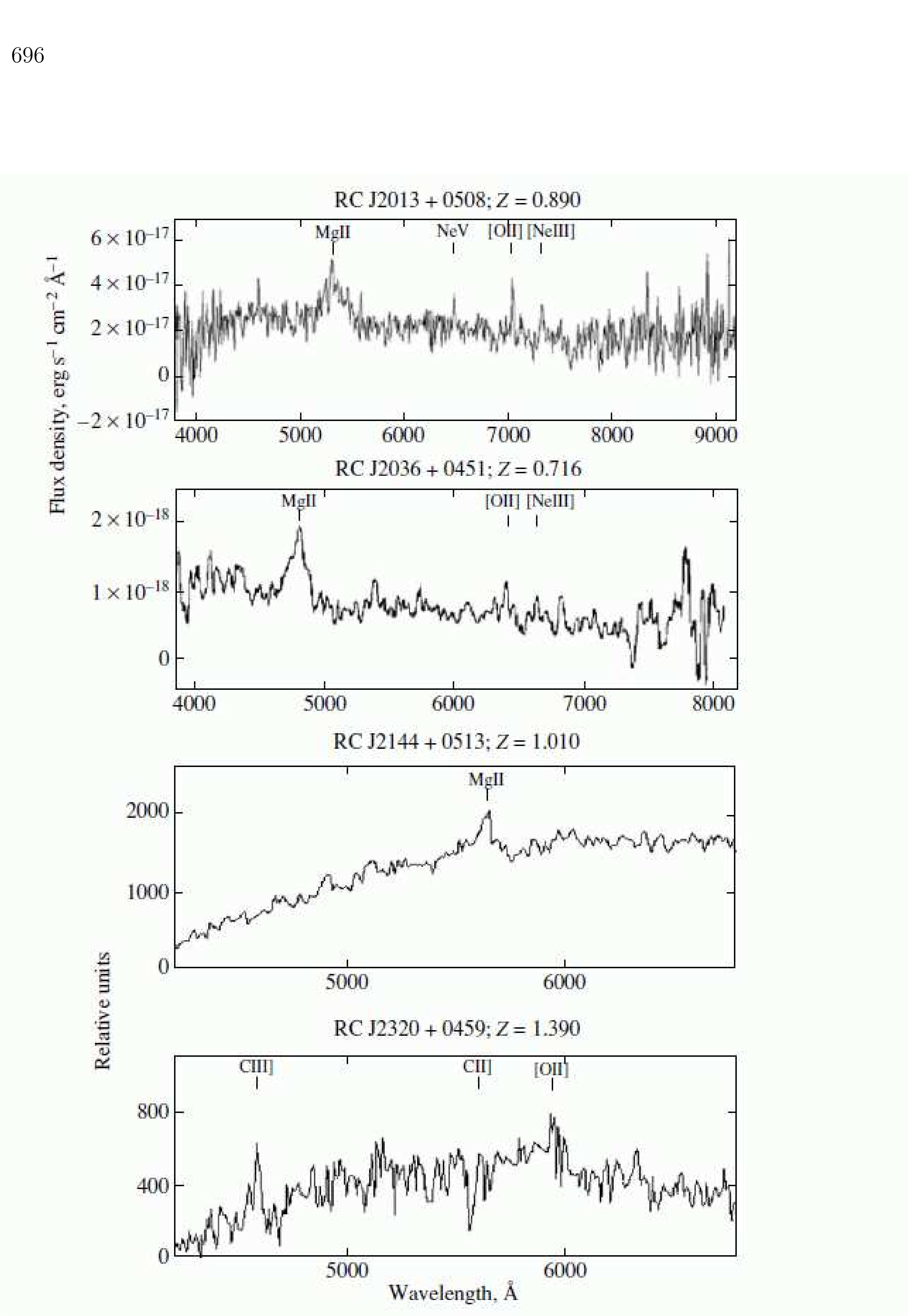

Fig. 3. (Continued)

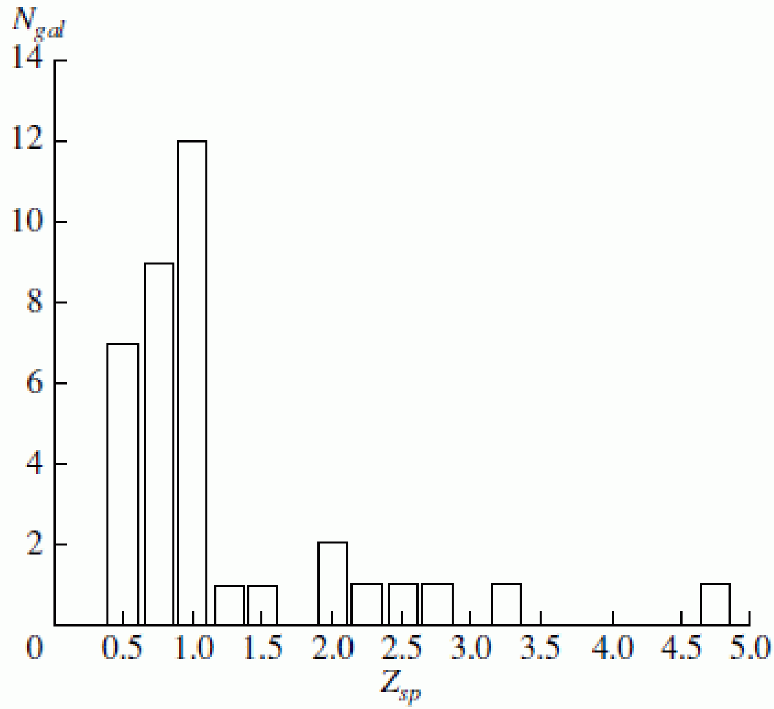

Figure 4: Redshift distribution of the galaxies.

made it possible to detect the object RCJ 0311+0507 with $z = 4.514$, which has a very high radio luminosity at centimeter wavelengths. Note that, since there are no selection effects, the fraction of distant objects in modern radio surveys (such as the NVSS) is much lower than the fraction in Fig. 4 resulting from the "Big Trio" program (see also the review by Pedani [29]). The identification of FRII radio sources at high redshifts is also helpful for searches for early "giant black holes" or first-generation clusters of galaxies.

We have presented here factual information on the 71 studied "Big Trio" objects. We are planning to discuss astrophysical implications of these data in future publications.

Acknowledgments

This study was partially supported by the Russian Foundation for Basic Research (project nos. 08-02-00486a, 09-07-00320) and the Program of State Support of Leading Scientific Schools of the Russian Federation. The authors thank the observers at the 6-m telescope of the SAO who performed the observations with the "Scorpio" spectrograph. The Very Large Array of the National Radio Astronomy Observatory is a Facility of the National Science Foundation operated under cooperative agreement by Associated Universities, Inc., a science management corporation.

References

[1]. W. M. Goss, Y. N. Parijskij, A. I. Kopylov, et al., Turkish J. Phys. **18**, 894 (1994).

[2]. O. V. Verkhodanov and Yu. N. Parijskij, Radio Galaxies and Cosmology (Fizmatlit, Moscow, 2009) [in Russian].

[3]. Y. N. Parijskij and D. V. Korolkov, Astrophys. Space Phys. Rev. **5**, 40 (1986).

[4]. Yu. N. Parijskij and D. V. Korolkov, Soobshch. Spets. Astrofiz. Observ. **12**, 5 (1984).

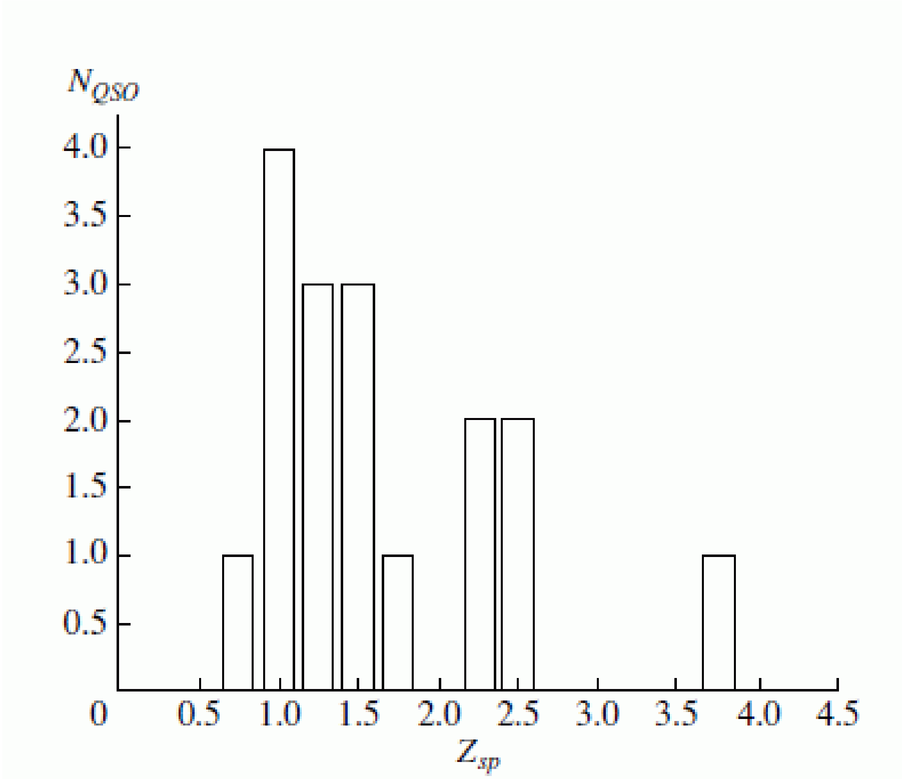

Figure 5: Redshift distribution of the quasars.

[5]. Yu. N.Parijskij, N.N. Bursov, N. M. Lipovka, et al., Astron. Astrophys. Suppl. Ser. **87**, 1 (1991).
[6]. Yu. N.Parijskij, N.N. Bursov, N. M. Lipovka, et al., Astron. Astrophys. Suppl. Ser. **96**, 583 (1992).
[7]. V. K. Kapahi andV.K.Kulkarni, Astron.J. **99**, 1397 (1990).
[8]. P. J. McCarthy, Ann. Rev. Astron. Astrophys. **31**, 639 (1993).
[9]. A. I. Kopylov, W. M. Goss, Yu. N. Parijskij, et al., Astron. Zh. **72**, 613 (1995) [Astron. Rep. **39**, 543 (1995)].
[10]. Yu.N.Parijskij, W.M. Goss, A. I. Kopylov, et al., Astron. Zh. **75**, 483 (1998) [Astron. Rep. **42**, 425 (1998)].
[11]. T. Pursimo, K. Nilson, P. Teerikorpi, et al., Astron. Astrophys. Suppl. Ser. **134**, 505 (1999).
[12]. O. V. Verkhodanov, A. I. Kopylov, Yu. N. Parijskij, et al., Astron. Zh. **79**, 589 (2002) [Astron. Rep. **46**, 531 (2002)].
[13]. O. V. Verkhodanov, Yu.N.Parijskij, N.S.Soboleva, et al., Bull. Spec. Astrophys. Observ. **52**, 5 (2001).
[14]. S. N. Dodonov, Yu.N.Parijskij, W. M.Goss, et al., Astron. Zh. **76**, 323 (1999) [Astron. Rep. **43**, 275 (1999)].
[15]. V. L. Afanasiev, S. N. Dodonov, A. V. Moiseev, et al., Astron. Zh. **80**, 409 (2003) [Astron. Rep. **47**, 377 (2003)].
[16]. W. M. Goss, Yu. N. Parijskij, N. S. Soboleva, et al., Astron. Zh. **69**, 673 (1992) [Sov. Astron. **36**, 343 (1992)].
[17]. Yu. N. Parijskij, W. M. Goss, A. I. Kopylov, et al., Bull. Spec.Astrophys.Observ. **40**, 5 (1996).
[18]. Yu. N. Parijskij, W. M. Goss, A. I. Kopylov, et al., Bull. Spec.Astrophys.Observ. **40**, 1 (1996).
[19]. Yu.N.Parijskij, W.M. Goss, A. I. Kopylov, et al., Astron. Astrophys. Trans. **18**, 437 (1999).
[20]. Yu. N. Parijskij, N. S. Soboleva, A. I. Kopylov et al., Pisma Astron. Zh. **26**, 493 (2000) [Astron.

Lett. **26**, 423 (2000)].
[21]. N. S. Soboleva, W. M. Goss, O. V. Verkhodanov, et al., Pisma Astron. Zh. **26**, 723 (2000) [Astron. Lett. **26**, 623 (2000)].
[22]. Yu.N.Parijskij, W.M.Goss, A. I. Kopylov, et al., Astron. Astrophys. Trans. **19**, 297 (2000).
[23]. Yu.N.Parijskij, N.S. Soboleva, W. M. Goss, et al., in Extragalactic Radio Sources, Ed. by R. Ekers et al. (Dordrecht, 1995), p. 591.
[24]. T. Pursimo, K. Nilson, P. Teerikorpi, et al., in Proc. of the 8th Russ.–Finn. Symp. on Astronomy (St. Petersburg, 1999), p. 95.
[25]. A. I. Kopylov, V. M. Goss, and Yu. N. Parijskij, Pisma Astron. Zh. **32**, 483 (2006) [Astron. Lett. **32**, 433 (2006)].
[26]. Yu.N.Parijskij, N.S.Soboleva, A. V. Temirova, and A. I. Kopylov, Astron. Zh. **71**, 821 (1994) [Astron. Rep. **38**, 731 (1994)].
[27]. A. I. Kopylov, Yu.N.Parijskij, N.S.Soboleva, et al., in Galaxy Evolution across the Hubble Time,Ed. by F. Combes and J. Palous (Cambridge Univ., Cambridge, 2007), p. 431.
[28]. G. Miley and C. de Breuck, Astron. Astrophys. Rev.**15**, 67 (2008).
[29]. M. Pedani, New Astron. **8**, 805 (2003).

Translated by N. Samus.